ESAIM: MODÉLISATION MATHÉMATIQUE ET ANALYSE NUMÉRIQUE

NATHALIE BARTOLI
FRANCIS COLLINO

Integral equations via saddle point problem for 2D electromagnetic problems

ESAIM: Modélisation mathématique et analyse numérique, tome 34, n° 5 (2000), p. 1023-1049

<http://www.numdam.org/item?id=M2AN_2000__34_5_1023_0>

Mathematical Modelling and Numerical Analysis
Modelisation Mathematique et Analyse Numerique

ESAIM M2AN
Vol 34, N° 5, 2000, p 1023–1049

INTEGRAL EQUATIONS *VIA* SADDLE POINT PROBLEM FOR 2D ELECTROMAGNETIC PROBLEMS

NATHALIE BARTOLI[1, 2] AND FRANCIS COLLINO[1]

Abstract. A new system of integral equations for the exterior 2D time harmonic scattering problem is investigated This system was first proposed by B Després in [11] Two new derivations of this system are given one from elementary manipulations of classical equations, the other based on a minimization of a quadratic functional Numerical issues are addressed to investigate the potential of the method

Résumé. Un nouveau système d'équations intégrales est proposé pour la résolution des problèmes bidimensionnels de diffraction d'ondes harmoniques Ce systeme a été initialement présenté par B Despres dans [11] Deux nouvelles dérivations de ce système sont données ici la première est obtenue à partir de manipulations sur les opérateurs intégraux classiques, la deuxième repose sur la minimisation d'une fonctionnelle quadratique Des résultats expérimentaux sont présentes et analysent les potentialités de cette méthode

Mathematics Subject Classification. 45F15, 65R20, 78A25, 78A45

Received February 22, 2000 Revised June 5, 2000

1 INTRODUCTION

This paper deals with the scattering of a 2D time-harmonic electromagnetic wave by obstacles More particularly, our interest is focused on the determination of the far field pattern of the scattered wave (Radar Cross Section) The problem is classically described through an integral representation of the electromagnetic fields This representation uses currents flowing at the surface of the obstacles which can be determined using some integral equations After discretization the associated matrix is, in the best cases, symmetric but non-Hermitian So, no guarantee of convergence is available when iterative methods are used to solve the linear system This is why direct methods of Gauss type are usually proposed However, for high frequencies, the number of unknowns increases rapidly due to the necessary refinement of the mesh For very large problems, direct methods are not tractable and some iterative methods must be used In [11], B Després proposed a new system of integral equations with nice properties This system stems from the minimization of a functional under constraints and gives a real symmetric but non-coercive bilinear form It is the purpose of this paper to study this new system In [11], the derivation of the equations is rather involved We will show that they can be recovered very easily from some manipulations of the usual potentials Then, we will give another derivation, more closely related to the one proposed in [11] and constructed from the minimization of a quadratic functional This second approach

Keywords and phrases Integral equation, saddle point problems

[1] CERFACS, 42 Av G Coriolis, 31057 Toulouse, France

[2] UMR MIP INSA-CNRS-UPS, Insa de Toulouse, Departement de Genie Mathematique, Toulouse, France

intends to simplify the arguments given in [11]. It allows us to justify the presence of our additional unknown which could appear somewhat arbitrary in the first derivation. Finally, we will present some numerical results. The goal of these numerical experiments is more to validate the approach in various situations than to do an exhaustive study.

The present paper is organized as follows. First, we derive the new system for the model problem (absorbing-like boundary condition) from manipulations of the integral operators (Sect. 2). Secondly, the same system is obtained from minimization of a quadratic functional (Sect. 3). This approach allows us to justify the presence of the Lagrange multiplier among the unknowns. In Section 4 the system is modified with the introduction of a penalization parameter β. It is done to provide a tractable system after discretization. Then, the system is extended to problems with general impedance boundary condition (Sect. 5). Two iterative methods are presented to solve the system: a relaxed Jacobi and a preconditioned GMRES (Sect. 6). Finally, some numerical experiments are reported to investigate and validate the method.

2. A first derivation of the Integral Equation system

We consider the scattering of a TE electromagnetic wave in the two-dimensional case. The domain D^-, bounded by a regular curve Γ, corresponds to the scatterer. The unit normal ν is outwardly directed to the exterior domain D^+. The only non zero component of the magnetic field is denoted by v^+. The out-going scattered field is a solution of the Helmholtz Equation,

$$\begin{cases} \Delta v^+ + k^2 v^+ = 0 \text{ in } D^+ \\ \lim\limits_{|x|\to\infty} |x|^{1/2}(\partial_{|x|} v^+ - ikv^+) = 0. \end{cases} \tag{1}$$

In this section, we will assume an impedance condition at the boundary of the scatterer

$$\partial_\nu v^+_{|\Gamma} + ikv^+_{|\Gamma} = g. \tag{2}$$

We will consider more general boundary conditions in Section 5.

2.1. The derivation of the Integral Equation system

Using the classical theory of potentials, [4], any solution v^+ of system (1) can be represented

$$v^+(x) = -\tilde{S}(\partial_\nu v^+_{|\Gamma})(x) + \tilde{K}(v^+_{|\Gamma})(x) \quad x \in D^+, \tag{3}$$

where $\tilde{S}$ and $\tilde{K}$ are the single- and double-layer potential defined by

$$\begin{aligned} \tilde{S}\varphi(x) &= \int_\Gamma G(x,y)\,\varphi(y)\mathrm{d}s(y), \ x \notin \Gamma \\ \tilde{K}\varphi(x) &= \int_\Gamma \partial_{\nu_y} G(x,y)\,\varphi(y)\mathrm{d}s(y), \ x \notin \Gamma. \end{aligned} \tag{4}$$

The kernel G is the out-going Green's function for the Helmholtz equation ($H_0^{(1)}$ is the Hankel function of the first kind and of order 0),

$$G(x,y) = \frac{i}{4} H_0^{(1)}(k|x-y|). \tag{5}$$

This integral representation (3) is independent of the boundary condition (2) on Γ (this condition will be considered subsequently). It introduces two currents, namely the trace of v^+ and the trace of $\partial_\nu v^+$ on Γ. The two unknowns are noted by

$$u = v^+_{|\Gamma}, \quad \partial u = \partial_\nu v^+_{|\Gamma}. \tag{6}$$

With the help of the jump relations across the boundary Γ, [10], we obtain from (3) the following relations

$$\begin{cases} \dfrac{ku}{2} &= -S\partial u + Kku \\ \dfrac{\partial u}{2} &= -K'\partial u + Tku \end{cases} \tag{7}$$

where S, K, K' and T are the potentials projected on Γ. They are defined by

$$\begin{aligned} S\varphi(x) &= k \int_\Gamma G(x,y)\,\varphi(y)\mathrm{d}s(y), \ x \in \Gamma \\ K\varphi(x) &= \int_\Gamma \partial_{\nu(y)} G(x,y)\,\varphi(y)\mathrm{d}s(y), \ x \in \Gamma \\ K'\varphi(x) &= \int_\Gamma \partial_{\nu(x)} G(x,y)\,\varphi(y)\mathrm{d}s(y), \ x \in \Gamma \\ T\varphi(x) &= \frac{1}{k}\,\partial_{\nu(x)} \int_\Gamma \partial_{\nu(y)} G(x,y)\,\varphi(y)\mathrm{d}s(y), \ x \in \Gamma. \end{aligned} \tag{8}$$

Consequently, (7) is equivalent to the following system (Id is the identity operator)

$$\mathbf{C}\begin{bmatrix} ku \\ \partial u \end{bmatrix} = \begin{bmatrix} 0 \\ 0 \end{bmatrix} \tag{9}$$

where

$$\mathbf{C} = \begin{bmatrix} T & -K' - \frac{1}{2}Id \\ -K + \frac{1}{2}Id & S \end{bmatrix}. \tag{10}$$

Relation (9) has yielded profound insights into electromagnetic behavior. It says that every pair $(ku, \partial u)$ of functions on Γ does not necessarily correspond to the traces of some radiating electromagnetic field. To be such a trace, $(ku, \partial u)$ must lie in the kernel of the integral operator $\mathbf{C}$.

Once the first system written, we can derive other relations by considering kernel's expression. The kernel $G(x,y)$ can be split into real and imaginary parts

$$\begin{cases} G(x,y) &= -\dfrac{1}{4}Y_0(k|x-y|) + \dfrac{i}{4}J_0(k|x-y|) \\ &= -G_r(k|x-y|) \ + i\,G_i(k|x-y|), \end{cases} \tag{11}$$

where J_0 and Y_0 denote the Bessel and the Neumann functions of order 0. Following this decomposition, the potentials read

$$S = -S_r + iS_i, \ K = -K_r + iK_i, \ T = -T_r + iT_i. \tag{12}$$

At this stage, we introduce λ and $\partial\lambda$, a new pair of unknowns defined on the boundary

$$\lambda = \imath u, \quad \partial\lambda = \imath \partial u. \tag{13}$$

Substituting (12) and (13) into (9), we obtain

$$\mathbf{K} \begin{bmatrix} ku \\ \partial u \end{bmatrix} - \mathbf{M} \begin{bmatrix} k\lambda \\ \partial\lambda \end{bmatrix} = 0, \tag{14}$$

where

$$\mathbf{K} = \begin{bmatrix} T_r & -K_r' + \frac{1}{2}Id \\ -K_r - \frac{1}{2}Id & S_r \end{bmatrix} \text{ and } \mathbf{M} = \begin{bmatrix} T_\imath & -K_\imath' \\ -K_\imath & S_\imath \end{bmatrix}. \tag{15}$$

Since S_r and T_r are symmetric, $\mathbf{K}$ is related to its adjoint $\mathbf{K}^\star$ through

$$\mathbf{K}^\star - \mathbf{K} = \begin{bmatrix} 0 & -Id \\ Id & 0 \end{bmatrix} = \Pi. \tag{16}$$

Up to now, the boundary condition has not been used. As we said, we assume an impedance condition on Γ of the following form

$$\partial_\nu v^+_{|\Gamma} + \imath k v^+_{|\Gamma} = g. \tag{17}$$

We multiply (17) by $\imath$ and we obtain the two equivalent relations

$$\begin{cases} ku - \imath\partial u &= -\imath g \\ \partial u + \imath k u &= g \end{cases} \tag{18}$$

or, in terms of matrices

$$\begin{bmatrix} ku \\ \partial u \end{bmatrix} + \begin{bmatrix} 0 & -Id \\ Id & 0 \end{bmatrix} \begin{bmatrix} k\lambda \\ \partial\lambda \end{bmatrix} = \begin{bmatrix} -\imath g \\ g \end{bmatrix} = \tilde{g}. \tag{19}$$

Using relation (16), we deduce

$$\begin{bmatrix} ku \\ \partial u \end{bmatrix} - \mathbf{K} \begin{bmatrix} k\lambda \\ \partial\lambda \end{bmatrix} + \mathbf{K}^\star \begin{bmatrix} k\lambda \\ \partial\lambda \end{bmatrix} = \tilde{g}. \tag{20}$$

Now, multiplying (14) by $\imath$, we have

$$\mathbf{K} \begin{bmatrix} k\lambda \\ \partial\lambda \end{bmatrix} + \mathbf{M} \begin{bmatrix} ku \\ \partial u \end{bmatrix} = 0. \tag{21}$$

Hence,

$$\begin{bmatrix} ku \\ \partial u \end{bmatrix} + \mathbf{M} \begin{bmatrix} ku \\ \partial u \end{bmatrix} + \mathbf{K}^\star \begin{bmatrix} k\lambda \\ \partial\lambda \end{bmatrix} = \tilde{g}. \tag{22}$$

We will now proceed to the derivation of the matrix $\mathbf{M}$ from the far field operator in order to deduce some of its properties.

Let C be the unit circle, and $\hat{x}$ a direction on the circle. We define the far field operator following Colton-Kress's definition of the diffusion amplitude (up to a k factor, *cf.* [10] p. 66).

$$\begin{aligned}\mathbf{A}_\infty \begin{bmatrix} ku \\ \partial u \end{bmatrix} &= -k\sqrt{\frac{\imath}{8\pi k}} \int_\Gamma e^{-\imath k\hat{x}\cdot y} \partial_{\nu_y} u(y) - u(y)\partial_{\nu_y} e^{-\imath k\hat{x}\cdot y} \mathrm{d}\Gamma(y) \\ &= -k\sqrt{\frac{\imath}{8\pi k}} \int_\Gamma e^{-\imath k\hat{x}\cdot y} (\partial u(y) + \imath k u(y)\hat{x}.\nu(y)) \mathrm{d}\Gamma(y). \end{aligned} \tag{23}$$

Its adjoint is given by

$$\mathbf{A}_\infty^\star \gamma(y) = k\sqrt{\frac{\imath}{8\pi k}} \begin{bmatrix} \int_C \gamma(\hat{x}) e^{\imath k\hat{x}\cdot y} \hat{x}.\nu(y) \mathrm{d}\hat{x} \\ \imath \int_C \gamma(\hat{x}) e^{\imath k\hat{x}\cdot y} \mathrm{d}\hat{x} \end{bmatrix}. \tag{24}$$

We then have the following lemma.

Lemma 2.1. *The matrix* $\mathbf{M}$ *as given in* (15) *is symmetric positive definite and can be split up*

$$\int_C \mathbf{A}_\infty \begin{bmatrix} ku \\ \partial u \end{bmatrix} \overline{\mathbf{A}_\infty \begin{bmatrix} kv \\ \partial v \end{bmatrix}} \mathrm{d}\hat{x} = \int_\Gamma \mathbf{M} \begin{bmatrix} ku \\ \partial u \end{bmatrix} \overline{\begin{bmatrix} kv \\ \partial v \end{bmatrix}} \mathrm{d}\Gamma, \tag{25}$$

or equivalently

$$\mathbf{M} = \mathbf{A}_\infty^\star \mathbf{A}_\infty. \tag{26}$$

The proof is based on the Jacobi-Anger expansion and the addition theorem for Bessel functions. It is given in Appendix A. Finally, the system reads

$$\begin{cases} x + \mathbf{A}_\infty^\star \mathbf{A}_\infty x + \mathbf{K}^\star y = \tilde{g} \\ \mathbf{K}x - \mathbf{A}_\infty^\star \mathbf{A}_\infty y = 0, \end{cases} \tag{27}$$

where the two unknowns are

$$x = \begin{bmatrix} ku \\ \partial u \end{bmatrix} \quad \text{and} \quad y = \begin{bmatrix} k\lambda \\ \partial \lambda \end{bmatrix} \quad \text{linked by } y = \imath x. \tag{28}$$

2.2. The saddle point problem

At this point, we notice that system (27) involves only real operators and is symmetric. Furthermore, it is just the optimality conditions of a saddle point problem. To make this point precise, let us regularize $\mathbf{K}$, by using some smooth approximation of the kernel G_r (we perform this to overcome all the functional analysis difficulties) and introduce an additional unknown γ

$$\gamma = -\imath \mathbf{A}_\infty y. \tag{29}$$

As a result, system (27) is rewritten as follows

$$\begin{cases} x + \mathbf{A}_\infty^\star \mathbf{A}_\infty x + \mathbf{K}^\star y = \tilde{g} \\ \gamma + \imath \mathbf{A}_\infty y = 0 \\ \mathbf{K}x - \imath \mathbf{A}_\infty^\star \gamma = 0. \end{cases} \tag{30}$$

Let us define the Lagrangian

$$\mathcal{L}(x^\star,\gamma^\star,y^\star)=\frac{1}{2}\|x^\star\|^2+\frac{1}{2}\|\mathbf{A}_\infty x^\star\|^2+\frac{1}{2}\|\gamma^\star\|^2+\mathcal{R}e\langle\mathbf{K}x-i\mathbf{A}_\infty^\star\gamma^\star,y\rangle-\mathcal{R}e\langle g,\mathbf{b}x^\star\rangle, \tag{31}$$

where

$$\mathbf{b}\begin{bmatrix} ku \\ \partial u\end{bmatrix}=\partial u+iku \quad \text{and} \quad \mathbf{b}^\star g=\begin{bmatrix} -ig \\ g\end{bmatrix}. \tag{32}$$

We observe that (27) or (30) derives directly from the optimality conditions of the associated saddle point problem. The triplet (x,γ,y) composed of primal variables (x,γ) and Lagrange parameter y is the solution of:

$$(x,\gamma,y)=\min_{x^*,\gamma^*}\max_{y^*}\mathcal{L}(x^*,\gamma^*,y^*). \tag{33}$$

As far as saddle point problems are concerned, it is known that this problem is well posed if the inf-sup condition of Brezzi is satisfied, [6]. We do not intend to give a detailed mathematical analysis of the well-posedness of our system here (details can be found in [2], [9]) but only indicate the main results. A possible functional framework is the following. Given $\mathcal{X}=L^2(\Gamma)\times L^2(\Gamma)$, let

$$\mathcal{Y}=\{y\in\mathcal{X},\mathbf{K}^\star y\in\mathcal{X}\} \text{ and } \mathcal{T}=\mathcal{Y}/\text{Ker}\mathbf{K}^\star, \tag{34}$$

equipped with the norms

$$\begin{aligned}\|y\|_{\mathcal{Y}}&=\|y\|_{\mathcal{X}}+\|\mathbf{K}^\star y\|_{\mathcal{X}}\\ \|y\|_{\mathcal{T}}&=\inf_{y_0\in Ker\mathbf{K}^\star}\|y-y_0\|_{\mathcal{Y}}=\|\mathbf{K}^\star y\|_{\mathcal{X}}+\inf_{y_0\in Ker\mathbf{K}^\star}\|y-y_0\|_{\mathcal{X}}.\end{aligned} \tag{35}$$

It can be shown that for some constant C

$$\inf_{y\in\mathcal{T}}\sup_{x\in\mathcal{X}}\frac{(x,\mathbf{K}^\star y)_{\mathcal{X}}}{\|x\|_{\mathcal{X}}}\geq\frac{1}{2}, \quad \text{and} \quad \|\mathbf{A}_\infty y\|_{L^2(C)}\leq C\|y\|_{\mathcal{T}}. \tag{36}$$

These two properties ensure the well-posedness of system (27) in $\mathcal{X}\times\mathcal{T}$. The key point of the verification of the inf-sup condition lies in the fact that $\Pi\mathbf{K}$ is one of the Calderon's projector defined in [8], (in particular $(\Pi\mathbf{K})^2=\Pi\mathbf{K}$). The continuity of $\mathbf{A}_\infty$ in $\mathcal{T}$ is a direct consequence of the remarkable identity

$$\text{Ker }\mathbf{A}_\infty=\text{Ker }\mathbf{K}^\star. \tag{37}$$

Actually, each pair in both kernels can be identified to the traces of some solution of the Helmholtz equation posed in the interior domain D^-.

A consequence of this brief analysis is that y the second argument of the solution of the saddle point problem is not unique in $\mathcal{X}$ (we only have uniqueness for x): the Lagrange parameter y is only known up to an element of Ker $\mathbf{K}^\star$.

3. A second derivation of the Integral Equation system

The purpose of this section is to show how system (27) derives from the minimization of a quadratic functional. Indeed, the approach presented in the first section may well have puzzled the reader: a saddle point problem arises but we did not explain where it comes from. Here, we exhibit the saddle point problem associated to the Lagrangian function which has been defined in (31). This different approach has been introduced by Després in [11]. The presentation we give here is still different but the key point of the method is always the isometric lemma.

3.1. The minimization problem

Let $\mathcal{W}$ be the space defined by

$$\mathcal{W} := \left\{ \begin{array}{l} w \in H^1_{loc}(D^+);\ \Delta w + k^2 w = 0 \text{ in } D^+ \\ w_{|\Gamma} \in L^2(\Gamma);\ \partial_\nu w_{|\Gamma} \in L^2(\Gamma) \\ \lim\limits_{R\to+\infty} \dfrac{1}{R} \displaystyle\int_{|x|\le R} |w(x)|^2 \, \mathrm{d}x < +\infty \end{array} \right\}. \tag{38}$$

If $w \in \mathcal{W}$, it admits the following expansion at infinity

$$\left\{ \begin{array}{l} \lim\limits_{|x|\to\infty} w(x) = a(w;\hat{x}) \dfrac{e^{ik|x|}}{\sqrt{|x|}} + b(w;\hat{x}) \dfrac{e^{-ik|x|}}{\sqrt{|x|}} \\ \lim\limits_{|x|\to\infty} \dfrac{\partial w}{\partial |x|}(x) = ika(w;\hat{x}) \dfrac{e^{ik|x|}}{\sqrt{|x|}} - ikb(w;\hat{x}) \dfrac{e^{-ik|x|}}{\sqrt{|x|}}, \end{array} \right. \tag{39}$$

where $a(w;\hat{x})$ and $b(w;\hat{x})$ are in $L^2(\mathcal{C})$, $\hat{x} = \frac{x}{|x|}$. This result will be proved later with the expression of a and b, the convergence $w(x) \to w_\infty(x)$ holding in the sense of Morrey-Campanato [15]

$$\lim_{R\to\infty} \frac{1}{R} \int_{R\le|x|\le 2R} |w(x) - w_\infty(x)|^2 \, \mathrm{d}x = 0. \tag{40}$$

Note that w appears as the sum of an out-going wave and of an incoming wave. Generally, we are only interested in out-going (radiating) solutions. Nevertheless, observing that the non-Hermitian property of the usual integral equations comes from the Sommerfeld condition at infinity, we seek the solution of our Helmholtz problem in a larger set (relaxation of the condition at infinity). Let g denote some function in $L^2(\Gamma)$, we define the functional $I(w)$ for $w \in \mathcal{W}$ by

$$I(w) = \frac{1}{4} \int_\Gamma |\partial_{\nu_y} w(y) + ikw(y)|^2 \mathrm{d}\Gamma(y) + \frac{1}{4} \int_\Gamma |-\partial_{\nu_y} w(y) + ikw(y)|^2 \mathrm{d}\Gamma(y)$$

$$+ k^2 \int_{\mathcal{C}} |b(w;\theta)|^2 \mathrm{d}\theta + k^2 \int_{\mathcal{C}} |a(w;\theta)|^2 \mathrm{d}\theta - \Re e \int_\Gamma \overline{g}(y) \, (\partial_{\nu_y} w(y) + ikw(y)) \mathrm{d}\Gamma(y). \tag{41}$$

The relationship between this functional and the radiating solution of our Helmholtz problem is the following

Proposition 3.1. *The minimum of the function $I(w)$ over $\mathcal{W}$ is v^+, i.e.*

$$v^+ = \operatorname{Arg}\min_{w\in\mathcal{W}} I(w) \quad \textit{where} \quad \left\{ \begin{array}{l} \Delta v^+ + k^2 v^+ = 0 \\ \partial_\nu v^+_{|\Gamma} + ikv^+_{|\Gamma} = g \\ b(v^+;\theta) = 0. \end{array} \right. \tag{42}$$

(note that $b = 0$ is equivalent to the Sommerfeld condition at infinity satisfied by v^+). The proposition 3.1 means that it is possible to relax both the condition at infinity and the boundary condition, and to recover them through the minimization process. The condition at infinity is treated exactly like the boundary condition on Γ.

Remark 3.2. It can be proved that changing $-\Re e \int_\Gamma \overline{g}(y)\,(\partial_{\nu_y} w(y) + ikw(y))\mathrm{d}\Gamma(y)$ into $-\Re e \int_\Gamma \overline{g}(y)\,(\partial_{\nu_y} w(y) - ikw(y))\mathrm{d}\Gamma(y)$ makes it possible to calculate the (incoming) solution of:

$$\begin{cases} \Delta v^+ + k^2 v^+ = 0 \\ \partial_\nu v^+_{|\Gamma} - ik\hat{v}^+_{|\Gamma} = g \\ a(v^+;\theta) = 0. \end{cases}$$

The proof of the Proposition 3.1 is based on the isometry lemma which is given next.

Lemma 3.3. (Isometry lemma). *Let $w \in \mathcal{W}$, we have*

$$\int_\Gamma |\partial_{\nu_y} w(y) + ikw(y)|^2 \mathrm{d}\Gamma(y) + 4k^2 \int_C |b(w;\theta)|^2 \mathrm{d}\theta = \int_\Gamma |-\partial_{\nu_y} w(y) + ikw(y)|^2 \mathrm{d}\Gamma(y) + 4k^2 \int_C |a(w;\theta)|^2 \mathrm{d}\theta. \quad (43)$$

Proof. The proof proceeds on the following steps. We denote by B_r, the ball of radius r, and Ω_r is defined by the intersection between B_r and the exterior domain D^+. Let n be the outgoing normal on $\partial\Omega_r = \partial B_r \cup \Gamma$.

We start from the Helmholtz equation multiplied by the conjugate of w

$$0 = \int_{\Omega_r} \Delta w \bar{w} + k^2 w\bar{w}\,\mathrm{d}\Omega_r \;\; = \int_{\Omega_r} -|\nabla w|^2 + k^2|w|^2\,\mathrm{d}\Omega_r + \int_{\partial\Omega_r} \partial_n w\,\bar{w}. \quad (44)$$

Retaining the imaginary part of this expression we get

$$\Im m \int_{\partial\Omega_r} 4k\partial_n w\,\bar{w} = \int_{\partial\Omega_r} |-\partial_n w + ikw|^2 - |\partial_n w + ikw|^2 = 0. \quad (45)$$

As $\partial_n = -\partial_\nu$ on Γ and $\partial_n = \partial_r$ on ∂B_r, it follows from (45) that

$$\begin{cases} \int_\Gamma |\partial_\nu w + ikw|^2 + \int_{\partial B_r} |-\partial_r w + ikw|^2 = \\ \int_\Gamma |-\partial_\nu w + ikw|^2 + \int_{\partial B_r} |\partial_r w + ikw|^2. \end{cases} \quad (46)$$

We then take the mean value of this equality for r in the interval $[R, 2R]$, and we let R go to infinity. By using properties (39), we get

$$\lim_{R\to\infty} \frac{1}{R} \int_R^{2R} \int_{\partial B_r} |-\partial_r w + ikw|^2 = \frac{1}{R} \int_R^{2R} \int_0^{2\pi} |2ikb(w;\theta)\frac{e^{-\imath kr}}{\sqrt{r}}|^2 r\mathrm{d}\theta\mathrm{d}r = 4k^2 \int_C |b(w;\theta)|^2 \mathrm{d}\theta. \quad (47)$$

In the same way,

$$\lim_{R\to\infty} \frac{1}{R} \int_R^{2R} \int_{\partial B_R} |\partial_r w + ikw|^2 \;\; = \;\; 4k^2 \int_C |a(w;\theta)|^2 \mathrm{d}\theta. \quad (48)$$

As a result, (3.3) is deduced from (46), (47) and (48). □

Once the isometry lemma has been obtained, the minimization of $I(w)$ becomes straightforward. In $\mathcal{W}$ we have the equivalent expression for the functional

$$\begin{aligned} I(w) &= \frac{1}{2}\int_\Gamma |\partial_\nu w + ikw|^2 + 2k^2 \int_C |b(w;\theta)|^2 \mathrm{d}\theta - \Re e \int_\Gamma \overline{g}\,(\partial_\nu w + ikw) \\ &= \frac{1}{2}\int_\Gamma |\partial_\nu w + ikw - g|^2 + 2k^2 \int_C |b(w;\theta)|^2 \mathrm{d}\theta - \frac{1}{2}\int_\Gamma |g|^2. \end{aligned}$$

Now Proposition 3.1 is immediately deduced: the minimum of $I(w)$ is $-\frac{1}{2}\|g\|^2$ and is reached at $w = v^+$.

3.2. **Parametrization of space $\mathcal{W}$**

The main difficulty consists in finding a tractable parametrization of the elements of $\mathcal{W}$. Indeed belonging to $\mathcal{W}$ requires a specific behavior at infinity and some regularity for the traces on Γ. All the remaining work will be to exhibit an appropriate parametrization of the problem related to quantities defined at the surface of Γ. We start by extending w by zero into the interior domain D^-. We consider the isomorphism $\mathcal{I}$ from $\mathcal{W}$ to $\mathcal{I}(\mathcal{W}) = \tilde{\mathcal{W}}$ defined by

$$\mathcal{I}(w) = \tilde{w} = \begin{cases} w \text{ on } D^+ \\ 0 \text{ on } D^- \end{cases} \qquad \text{with } w \in \mathcal{W}. \tag{49}$$

It is straightforward to prove that $\tilde{w}$ satisfies in the sense of distributions of $\mathbb{R}^2$

$$\Delta\tilde{w} + k^2\tilde{w} = \nabla w \cdot \nu\, \delta_\Gamma + \mathrm{div}(w\nu\delta_\Gamma). \tag{50}$$

The general solution $\tilde{w} \in \tilde{\mathcal{W}}$ is made up of two terms, namely $\tilde{w}_H$, the solution of the homogeneous equation and $\tilde{w}_P$, some particular solution of the complete equation. As the second term is a distribution with compact support, a particular solution is

$$\tilde{w}_P = -\mathrm{Green} * (\nabla w \cdot \nu\, \delta_\Gamma + \mathrm{div}(w\nu\delta_\Gamma)) \tag{51}$$

where Green is some convex combination of out-going and incoming Helmholtz Green functions (one verifies that $\tilde{w}_P$ satisfies the growth property at infinity required to be in $\mathcal{W}$, see Sect. 3.3). As we do not dispose any radiation condition (out-going or incoming), the uniqueness of the solution can not be demonstrated. For that reason, we must consider the solution of the homogeneous system $\tilde{w}_H$: $\tilde{w}_H$ is a free wave which verifies

$$\begin{cases} \Delta\tilde{w}_H + k^2\tilde{w}_H = 0 \\ \lim\limits_{R\to\infty} \dfrac{1}{R}\displaystyle\int_{|x|\le R} |\tilde{w}_H(x)|^2 \,\mathrm{d}x < \infty. \end{cases} \tag{52}$$

By using Theorem 3.22 of [10], we know that $\tilde{w}_H$ is an Herglotz wave, *i.e.* there exists some $\gamma \in L^2(C)$ such that

$$\tilde{w}_H(\gamma;x) = \sqrt{\frac{i}{8\pi k}} \int_C \gamma(\theta) e^{ikx\theta} \mathrm{d}\theta, \tag{53}$$

the kernel γ is called the Herglotz kernel of $\tilde{w}_H$ and the factor $\sqrt{\frac{i}{8\pi k}}$ is just here for convenience. Finally, $\tilde{w}$ $(=\tilde{w}_P+\tilde{w}_H)$ is the general solution of Helmholtz equation (50) in $\mathbb{R}^2$ with the required behavior at infinity.

In our space of solution, we have considered both incoming and out-going solutions; for this reason, we choose the following Green's function

$$\text{Green}(x,y) = G_{Y_0}(x,y) = \frac{1}{2}(\frac{\imath}{4}H_0^{(1)}(k|x-y|) - \frac{\imath}{4}H_0^{(2)}(k|x-y|)) = -\frac{Y_0(k|x-y|)}{4}\,. \tag{54}$$

For $x \notin \Gamma$, the general solution reduces to

$$\tilde{w}(x) = \tilde{w}_P(kw_{|\Gamma}, \partial_\nu w_{|\Gamma}) + \tilde{w}_H(\gamma) \tag{55}$$

where $\tilde{w}_H$ is given by equation (53) and

$$\tilde{w}_P(kv, \partial v) = -\int_\Gamma G_{Y_0}(x.y)\partial v(y)\mathrm{d}\Gamma(y) + \frac{1}{k}\int_\Gamma \partial_{\nu_y} G_{Y_0}(x,y)kv(y)\mathrm{d}\Gamma(y). \tag{56}$$

So, $\tilde{w}(x)$ can be described by three variables: $kw|_\Gamma$, $\partial_\nu w|_\Gamma$ and $\gamma(\theta)$. Before using this parametrization, we must study $\tilde{w}(x)$ in D^-.

Let $(kv, \partial v, \gamma)$ in $L^2(\Gamma)^2 \times L^2(\mathcal{C})$ and the function $\tilde{w}$, such that

$$\tilde{w} = \tilde{w}(kv, \partial v, \gamma) = \tilde{w}_P(kv, \partial v) + \tilde{w}_H(\gamma).$$

It is easy to check that $\tilde{w}_{|_{D^+}} = w \in \mathcal{W}$. However, to identify the traces of $\tilde{w}$, we must impose $\tilde{w}$ vanishes in the interior domain, *i.e.* $\tilde{w}$ is in $\tilde{\mathcal{W}}$ (in other words, we need a parametrization of $\tilde{\mathcal{W}}$). To obtain that, it is enough to impose both conditions

$$\begin{cases} \lim\limits_{x \to x_0^-} \nabla\tilde{w}(x).\nu(x) = 0 \text{ and} \\ \lim\limits_{x \to x_0^-} k\tilde{w}(x) = 0 \text{ where } x_0 \in \Gamma \end{cases} \tag{57}$$

Indeed, since $\Delta\tilde{w} + k^2\tilde{w} = 0$ in D^-, boundary conditions (57) imply the solution vanishes in D^-. Using the jump relations for the potential layers, we can rewrite (57) as

$$\begin{cases} 0 &= -\displaystyle\int_\Gamma \partial_{\nu_x} G_{Y_0}(x,y)\partial v(y)\mathrm{d}\Gamma(y) + \sqrt{\frac{\imath}{8\pi k}}\imath k \int_{\mathcal{C}} \gamma(\theta) e^{\imath k x\theta}\theta.\nu(x)\mathrm{d}\theta \\ & \quad + \displaystyle\frac{1}{k\partial\nu(x)}\int_\Gamma \partial_{\nu_y} G_{Y_0}(x,y)kv(y)\mathrm{d}\Gamma(y) - \frac{1}{2}\partial v(x_0) \\ 0 &= -k\displaystyle\int_\Gamma G_{Y_0}(x,y)\partial v(y)\mathrm{d}\Gamma(y) + k\sqrt{\frac{\imath}{8\pi k}}\int_{\mathcal{C}} \gamma(\theta)e^{\imath k x\theta}\mathrm{d}\theta \\ & \quad + \displaystyle\int_\Gamma \partial\nu_y G_{Y_0}(x,y)kv(y)\mathrm{d}\Gamma(y) - \frac{1}{2}kv(x_0), \end{cases} \tag{58}$$

or in an equivalent way, multiplying the first equation by -1 and using both matrices defined in (15), (24) and $G_{Y_0} = -G_r$

$$\mathbf{K}\begin{bmatrix} kv \\ \partial v \end{bmatrix} - \imath\mathbf{A}_\infty^\star\gamma = 0. \tag{59}$$

In conclusion, the triplets $(kv, \partial v, \gamma)$ in $L^2(\Gamma)^2 \times L^2(\mathcal{C})$ which satisfy the constraint (59) are a parametrization of $\tilde{\mathcal{W}}$. Every such triplet is associated through (55) to a solution of the Helmholtz equation whose exterior traces on Γ coincide with $(kv, \partial v)$.

3.3. The asymptotic analysis

Now, our attention is focused on the asymptotic behavior of functions of $\tilde{\mathcal{W}}$, *i.e.* the achievement of the existence of some $a(\tilde{w})$ and $b(\tilde{w})$ such that

$$\lim_{|x|\to\infty} \tilde{w}(x) = a_\infty(w;\hat{x})\frac{e^{\imath k|x|}}{\sqrt{|x|}} + b_\infty(w;\hat{x})\frac{e^{-\imath k|x|}}{\sqrt{|x|}}. \tag{60}$$

We start with the classical potentials. Using the asymptotics of Hankel functions for large argument, *cf.* page 65 in [10], we get

$$\int_\Gamma G_{Y_0}(x,y)\partial_\nu v(y)\mathrm{d}\Gamma(y) = \left(a_P^1(\hat{x})\frac{e^{\imath k|x|}}{\sqrt{|x|}} + b_P^1(\hat{x})\frac{e^{-\imath k|x|}}{\sqrt{|x|}}\right)\left(1+O(\frac{1}{|x|})\right), \tag{61}$$

$$\text{where } \begin{cases} a_P^1(\hat{x}) = \sqrt{\dfrac{i}{32\pi k}}\displaystyle\int_\Gamma e^{-\imath k\hat{x}y}\partial v(y)\mathrm{d}\Gamma(y) \\ b_P^1(\hat{x}) = -ia_P^1(-\hat{x}) \end{cases} \tag{62}$$

and

$$\int_\Gamma \partial_\nu G_{Y_0}(x,y)v(y)\mathrm{d}\Gamma(y) = \left(a_P^2(\hat{x})\frac{e^{\imath k|x|}}{\sqrt{|x|}} + b_P^2(\hat{x})\frac{e^{-\imath k|x|}}{\sqrt{|x|}}\right)\left(1+O(\frac{1}{|x|})\right) \tag{63}$$

$$\text{where } \begin{cases} a_P^2(\hat{x}) = -i\sqrt{\dfrac{i}{32\pi k}}\displaystyle\int_\Gamma e^{-\imath k\hat{x}y}\hat{x}.\nu k v(y)\mathrm{d}\Gamma(y) \\ b_P^2(\hat{x}) = -ia_P^2(-\hat{x}). \end{cases} \tag{64}$$

For a Herglotz wave with a regular γ, the asymptotic behavior can be obtained by means of the stationary phase theorem

$$w_H(x) \to w_H^{asy}(x) = \frac{\gamma(\hat{x})}{2k}\frac{e^{\imath kx}}{\sqrt{|x|}} + \frac{i\gamma(-\hat{x})}{2k}\frac{e^{-\imath kx}}{\sqrt{|x|}},\ |x|\to\infty. \tag{65}$$

For $\gamma \in C^1(\mathcal{C})$, the convergence is pointwise

$$w_H(\gamma;x) = w_H^{asy}(\gamma;x)\left(1+\mathcal{O}(\frac{\|\gamma\|_{C^1}}{|x|})\right). \tag{66}$$

In Appendix B, this result is extended to a more general Herglotz kernel γ in L^2: as a result, with only the regularity L^2, convergence is found to hold only in the weak sense (40). Note that this convergence is sufficient to derive the isometry Lemma 3.3.

Finally, we sum all these asymptotic contributions to identify the expressions of $a_\infty(w;\hat{x})$ and $b_\infty(w;\hat{x})$.

$$a_\infty(w;\hat{x}) = \frac{1}{2k}\left(\mathbf{A}_\infty\begin{bmatrix} kv \\ \partial v\end{bmatrix}(\hat{x}) + \gamma(\hat{x})\right) \tag{67}$$

$$b_\infty(w;\hat{x}) = \frac{-i}{2k}\left(\mathbf{A}_\infty\begin{bmatrix} kv \\ \partial v\end{bmatrix}(-\hat{x}) - \gamma(-\hat{x})\right), \tag{68}$$

and

$$\begin{cases} a_\infty(w;\hat{x}) + ib_\infty(w;-\hat{x}) = \dfrac{1}{k}\mathbf{A}_\infty \begin{bmatrix} kv \\ \partial v \end{bmatrix} \quad (\hat{x}) \\ a_\infty(w;\hat{x}) - ib_\infty(w;-\hat{x}) = \dfrac{1}{k}\gamma(\hat{x}). \end{cases} \tag{69}$$

3.4. The saddle point formulation

At this point in the presentation, we have managed to express $a_\infty(w;\hat{x})$ and $b_\infty(w;\hat{x})$ as functions of the three parameters $(kv, \partial v, \gamma)$. Now, the expression of the functional will be readily derived.

On one hand, from (69) we have

$$k^2 \int_C |a(w;\hat{x})|^2 \mathrm{d}\hat{x} + k^2 \int_C |b(w;\hat{x})|^2 \mathrm{d}\hat{x} = \frac{1}{2}\int_C |\gamma(\hat{x})|^2 \mathrm{d}\hat{x} + \frac{1}{2}\int_C |\mathbf{A}_\infty(kv, \partial v;\hat{x})|^2 \mathrm{d}\hat{x}, \tag{70}$$

and on the other hand

$$\begin{aligned} \frac{1}{4}\int_\Gamma |-\partial_{\nu_y} w(y) + ikw(y)|^2 \mathrm{d}\Gamma(y) + \frac{1}{4}\int_\Gamma |\partial_{\nu_y} w(y) + ikw(y)|^2 \mathrm{d}\Gamma(y) &= \frac{1}{2}\int_\Gamma |\partial_{\nu_y} w(y)|^2 + |kw(y)|^2 \mathrm{d}\Gamma(y) \\ &= \frac{1}{2}\int_\Gamma |\partial v(y)|^2 + |kv(y)|^2 \mathrm{d}\Gamma(y). \end{aligned} \tag{71}$$

We finally obtain

$$\begin{cases} I(w) = I(kv, \partial v, \gamma) = \dfrac{1}{2}\displaystyle\int_\Gamma |\partial v(y)|^2 + |kv(y)|^2 \mathrm{d}\Gamma(y) \\ \quad + \dfrac{1}{2}\displaystyle\int_C |\gamma(\hat{x})|^2 \mathrm{d}\hat{x} + \frac{1}{2}\int_C |\mathbf{A}_\infty(kv, \partial v;\hat{x})|^2 \mathrm{d}\hat{x} \\ \quad - \Re\mathrm{e}\displaystyle\int_\Gamma g\,\overline{(\partial v(y) + ikv(y))}\,\mathrm{d}\Gamma(y). \end{cases} \tag{72}$$

This expression allows us to rewrite Proposition 3.1 as follows:

Proposition 3.4. *Let*

$$\mathcal{M} = \left\{ \begin{array}{c} \mu = (kv,\ \partial v,\ \gamma) \in L^2(\Gamma) \times L^2(\Gamma) \times L^2(C) \\ \textit{so that } \mathbf{K} \begin{bmatrix} kv \\ \partial v \end{bmatrix} - i\mathbf{A}_\infty^\star \gamma = 0, \end{array} \right\}, \tag{73}$$

the solution $\tilde{\mu}$ *of*

$$\tilde{\mu} = (\tilde{kv},\ \tilde{\partial v},\ \tilde{\gamma}) = \quad \mathrm{Arg}\min_{\mu\in\mathcal{M}} \quad I(\mu), \tag{74}$$

is given by

$$\tilde{kv} = kv^+_{|\Gamma} \quad \tilde{\partial v} = \partial_\nu v^+_{|\Gamma} \quad \tilde{\gamma} = ka_\infty(v^+;\hat{x}), \tag{75}$$

where v^+ *is the solution of*

$$\begin{cases} \Delta v^+ + k^2 v^+ = 0 \\ \partial_\nu v^+_{|\Gamma} + ikv^+_{|\Gamma} = g \\ v^+(x) \sim a_\infty(v^+;\hat{x})\dfrac{e^{ik|x|}}{\sqrt{|x|}},\ |x| \to \infty. \end{cases} \tag{76}$$

To solve this constrained minimization problem (73)-(74), it is classical to introduce the Lagrangian function,

$$\begin{aligned} \mathcal{L}(x^\star,\gamma^\star,y^\star) = \frac{1}{2}\|x^\star\|^2 + \frac{1}{2}\|\mathbf{A}_\infty x^\star\|^2 + \frac{1}{2}\|\gamma^\star\|^2 \\ -\mathcal{R}e\langle g, \mathbf{b}x^\star\rangle + \mathcal{R}e\langle \mathbf{K}x^\star - i\mathbf{A}^\star_\infty\gamma^\star, y^\star\rangle. \end{aligned} \tag{77}$$

It is well known that if the Lagrangian admits a saddle point, then it is the minimum argument of

$$\mathcal{L}(x,\gamma,y) = \min_{w^\star\in\mathcal{W}} I(w^\star). \tag{78}$$

The optimality conditions are deduced from

$$\frac{\partial\mathcal{L}}{\partial x} = \frac{\partial\mathcal{L}}{\partial y} = \frac{\partial\mathcal{L}}{\partial\gamma} = 0.$$

Finally, we obtain

$$\begin{cases} x + \mathbf{A}^\star_\infty\mathbf{A}_\infty x + \mathbf{K}^\star y = \tilde{g} \\ \gamma + i\mathbf{A}_\infty y = 0 \\ \mathbf{K}x - i\mathbf{A}^\star_\infty\gamma = 0. \end{cases} \tag{79}$$

The elimination of γ in (79) reduces the system to (27).

Conclusion. The system (27) may be perfectly studied thanks to the introduced functional spaces. Yet, it is useful to consider the second derivation to get a better understanding of the underlying minimization problem. It is therefore not surprising that system (79) is similar to the initial system of Després in [11].

4. A MODIFICATION: THE β-SYSTEM

A difficulty arises with the use of $(\mathcal{X},\mathcal{T})$ spaces when discretization is considered. Indeed, space $\mathcal{T}$ possesses a complicate structure and it is difficult to find a suitable discretization to satisfy the discrete uniform inf-sup condition. To avoid that, Després suggests us (in a personal communication) to modify the system, using the fact that $y = ix$. The new system does not correspond any more to a saddle point problem but has nice coercive properties.

Let β be some positive parameter (for instance $\beta = 1$). Since $y = ix$, we add to system (27)

$$\begin{array}{ll} \beta x = -i\beta y & \text{in the first equation and} \\ \beta y = i\beta x & \text{in the second one.} \end{array} \tag{80}$$

The new system is

$$\begin{cases} (Id+\beta)x + \mathbf{A}^\star_\infty\mathbf{A}_\infty x + \mathbf{K}^\star y + i\beta y = \tilde{g} \\ -\mathbf{K}x + (\beta + \mathbf{A}^\star_\infty\mathbf{A}_\infty)y - i\beta x = 0, \end{cases} \tag{81}$$

or, in an equivalent form

$$\mathcal{M}_\beta \begin{bmatrix} x \\ y \end{bmatrix} = \begin{bmatrix} \tilde{g} \\ 0 \end{bmatrix}. \tag{82}$$

A simple calculation shows that the coercivity is ensured:

$$\Re e\left(\mathcal{M}_\beta \begin{pmatrix} x \\ y \end{pmatrix}, \begin{pmatrix} x \\ y \end{pmatrix}\right)_{\mathcal{X}\times\mathcal{X}} = \|x\|^2_{\mathcal{X}} + \beta\|x+iy\|^2_{\mathcal{X}} + \|\mathbf{A}_\infty x\|^2 + \|\mathbf{A}_\infty y\|^2 \geq \min(\frac{\beta}{2}, \frac{1}{3})(\|x\|^2_{\mathcal{X}} + \|y\|^2_{\mathcal{X}}).$$

5. The system for a general impedance condition

The Després's system (27) has been written for the impedance condition (17). To extend it to more general boundary conditions we consider the problem

$$\begin{cases} \Delta v^+ + k^2 v^+ = 0 \text{ in } D^+ \\ \lim\limits_{|x|\to\infty} |x|^{1/2}(\partial_r v^+ - ikv^+) = 0 \\ \partial_\nu v^+ + ik\mathcal{Z}v^+ = F \text{ on } \Gamma, \end{cases} \tag{83}$$

where $\mathcal{Z}$ can be a pure constant, or more generally some operators (differential, pseudo-differential, ... [3–5]) acting on a function defined on the boundary. To have a well posed problem, we assume the impedance operator $\mathcal{Z}$ has a positive real part. Associated to $\mathcal{Z}$ is the reflection operator $\mathcal{R}$ defined by

$$\mathcal{R} = \frac{Id - \mathcal{Z}}{Id + \mathcal{Z}}. \tag{84}$$

The assumption on $\mathcal{Z}$ implies $\|\mathcal{R}\| \leq 1$. The well-known boundary conditions follow directly from particular values of $\mathcal{Z}$:

- if $\mathcal{Z} = 0$ (R=1), we get the Neumann boundary condition

$$\partial_\nu v^+ = F \text{ on } \Gamma$$

- if $\mathcal{Z} \to \infty$ (R=-1), the Dirichlet boundary condition is deduced

$$v^+ = 0 \text{ on } \Gamma.$$

We have already treated the problem with the condition given by

$$\partial_\nu v^+ + ikv^+ = g.$$

The right hand side g can be expressed in terms of $\mathcal{R}$ through

$$g = \mathcal{R}(-\partial_\nu v + ikv) + (1+\mathcal{R})F. \tag{85}$$

Combining the definition of $\tilde{g}$ given by (19) and the new expression for g, we deduce

$$\begin{cases} x + \mathbf{A}^\star_\infty \mathbf{A}_\infty x + \mathbf{K}^\star y = N_{\mathcal{R}} x + f \\ \mathbf{K}x - \mathbf{A}^\star_\infty \mathbf{A}_\infty y = 0, \end{cases} \tag{86}$$

where

$$f = \begin{bmatrix} -i(1+\mathcal{R})F \\ (1+\mathcal{R})F \end{bmatrix}, \tag{87}$$

and

$$N_{\mathcal{R}}x = N_{\mathcal{R}} \begin{bmatrix} ku \\ \partial u \end{bmatrix} = \begin{bmatrix} -i\mathcal{R}(-\partial u + iku) \\ \mathcal{R}(-\partial u + iku) \end{bmatrix}. \tag{88}$$

We modify the system by adding terms in β as previously, and we obtain

$$\begin{cases} (Id+\beta)x + \mathbf{A}_\infty^\star \mathbf{A}_\infty x + \mathbf{K}^\star y = N_{\mathcal{R}}x + f - i\beta y \\ \mathbf{K}x - (\beta + \mathbf{A}_\infty^\star \mathbf{A}_\infty)y = -i\beta x. \end{cases} \tag{89}$$

Schematically, this system reads

$$\mathcal{C}_\beta \begin{bmatrix} x \\ y \end{bmatrix} = \mathcal{R}_{\mathcal{R},\beta} \begin{bmatrix} x \\ y \end{bmatrix} + \begin{bmatrix} f \\ 0 \end{bmatrix} \tag{90}$$

with

$$\mathcal{C}_\beta = \begin{bmatrix} (1+\beta)Id + \mathbf{A}_\infty^\star \mathbf{A}_\infty & \mathbf{K}^\star \\ \mathbf{K} & -(\beta + \mathbf{A}_\infty^\star \mathbf{A}_\infty) \end{bmatrix} \tag{91}$$

and

$$\mathcal{R}_{\mathcal{R},\beta} = \begin{bmatrix} N_{\mathcal{R}} & -i\beta \\ -i\beta & 0 \end{bmatrix}. \tag{92}$$

6. Some iterative algorithms

To cope with system (89), several iterative methods can be imagined. The simplest is a relaxed Jacobi method based on the splitting $(\mathcal{C}_\beta, \mathcal{R}_{\mathcal{R},\beta})$. Let r be the relaxation parameter. The iterative algorithm is

- computation of f *via* (87);
- initialization: $x^0 = 0$ and $y^0 = 0$;
- iterate over p, the iteration index:
  - solve

$$\mathcal{C}_\beta \begin{bmatrix} \tilde{x}^p \\ \tilde{y}^p \end{bmatrix} = \mathcal{R}_{\mathcal{R},\beta} \begin{bmatrix} x^{p-1} \\ y^{p-1} \end{bmatrix} + \begin{bmatrix} f \\ 0 \end{bmatrix} \tag{93}$$

  - relax

$$x^p = (1-r)x^{p-1} + r\tilde{x}^p, \quad y^p = (1-r)y^{p-1} + r\tilde{y}^p. \tag{94}$$

When $\mathcal{R}$ is a scalar number, the convergence of this algorithm is proved provided that

$$\|\mathcal{R}\| \leq 1 \quad \text{and} \quad 0 < r < 1. \tag{95}$$

If $\|\mathcal{R}\| \neq 1$, this convergence is strong ($\|x^p - x\|_{\mathcal{X}} \to 0$ where (x, y) is the sought solution), otherwise it is weak ($x^p \to x$ weakly in $\mathcal{X}$). In all cases the far fields $\mathbf{A}_\infty(y^p - y)$ and $\mathbf{A}_\infty(x^p - x)$ tend strongly to zero in $L^2(\mathcal{C})$.

The proof is quite similar to the case of Maxwell's problem developed in [9] and will not be reproduced here. For a more general framework where $\mathcal{R}$ is an operator, the reader is referred to [2].

A more sophisticated approach is to apply a GMRES algorithm to the system

$$\begin{bmatrix} x \\ y \end{bmatrix} - (\mathcal{C}_\beta)^{-1} \left(\mathcal{R}_{\mathcal{R},\beta} \begin{bmatrix} x \\ y \end{bmatrix} + \begin{bmatrix} f \\ 0 \end{bmatrix} \right) = 0. \tag{96}$$

The theory of GMRES is described in [16] and one of its implementations in [12]. We do not have any theoretical result about the convergence of this method when the restart parameter is lower than the size of the problem. However, we will see its efficiency during the numerical experiments.

7. Numerical experiments

7.1. Discretization of boundary integral equations

First and foremost, the integral system is rewritten through a variational formulation in order to involve only weakly singular integrals, *cf.* [5] for more details. For instance, derivative of the double layer potential is removed and the new formulation is given by

$$\int_\Gamma (\partial_{\nu_x} T_r \phi)(x(s))\, \phi^t(x(s)) \mathrm{d}\Gamma(s) = -\frac{1}{k^2} \int_\Gamma S_r(\partial_s \phi)(x(s))\, \partial_s \phi^t(x(s))\, \mathrm{d}\Gamma(s) + \int_\Gamma S_r(\phi\nu)(x(s)) \cdot (\phi^t \nu)(x(s))\, \mathrm{d}\Gamma(s).$$

A Galerkin method is used: the boundary is split into segments and all functions (both unknowns and test functions) are approximated by $\mathcal{C}^0$ finite elements (only differential operators of order at most 1 occur). For distant pairs of segments, the double integrals are approximated by means of a two point Gauss-Legendre quadrature formula, whereas the nearest elements receive special attention. The numerical integration is done *via* extraction and exact integration of singularities like $\log|x-y|$, $\partial_{\nu_x} \log|x-y|$. Concerning the operator $\mathbf{M}$, the associated matrix is calculated from (26) and the following Fourier series expansion suitably truncated (this series also called the Jacobi-Anger expansion is introduced in Appendix A, p. 26)

$$e^{-ik\hat{x}.y} = \sum_{\ell=-\infty}^{+\infty} (-i)^\ell J_\ell(k|y|) e^{i\ell(\theta_y - \theta_{\hat{x}})}. \tag{97}$$

The number of modes is fixed by

$$|\ell| \leq N_\ell, \ N_\ell = \max\left(kD + 6\log(kD+\pi), 10\right)$$

where D is the half of the scatterer diameter.

7.2. Solution of system (93)

When system (93) is solved by the Jacobi algorithm with relaxation process, at each Jacobi iterative step, the couple $(\tilde{x}^p, \tilde{y}^p)$ has to be determined *via* some second iterative procedure. Due to the symmetric nature of operator $\mathcal{C}_\beta$, different algorithms are available, for instance SymmLQ [14], Double Conjugate Gradient (DbleCG) [13] or OrthoCG [7]. These three methods will be compared. Let us recall that DbleCG consists in solving the matricial system

$$\begin{bmatrix} \mathbb{M}_1 & \mathbb{K}^\star \\ \mathbb{K} & -\mathbb{M}_2 \end{bmatrix} \begin{bmatrix} x \\ y \end{bmatrix} = \begin{bmatrix} f \\ g \end{bmatrix} \tag{98}$$

or equivalently

$$\begin{cases} \left(\mathbb{K}\mathbb{M}_1^{-1}\mathbb{K}^\star + \mathbb{M}_2\right) y = \mathbb{K}\mathbb{M}_1^{-1} f - g \\ \mathbb{M}_1 x = f - \mathbb{K}^\star y \end{cases} \tag{99}$$

by using Conjugate Gradient (CG) methods: a first CG is used to solve the system in y and, at each iteration, a second CG is used to invert $\mathbb{M}_1$.

7.3. Circular geometry

In our first example, the method is validated on a circular geometry. Indeed, in this particular case, computed currents and the Radar Cross Section (RCS) can be compared with exact values from Fourier series.

The parameter β, which has been introduced in (80) is crucial for the convergence of the iterative algorithm. If $\beta = 0$, the iterative system converges to a solution polluted by elements in the kernel of $\mathbf{K}^\star$. Unlike the continuous model, the matrix associated with the discrete system is ill-conditioned and the inf-sup condition is not satisfied any more. Conversely, if $\beta = 1$, the exact and computed currents fit. Below the relative RCS error (expressed as a percentage) are reported for either the Neumann problem ($\mathcal{R} = 1$) or a model problem ($\mathcal{R} = 0$). The unit circle is discretized with 50 or 100 points and k is picked equal to 2. The tolerance criterium for Jacobi equals 10^{-5}.

Unit circle, $k = 2$	with 50 points		with 100 points	
	Neumann pb	model pb	Neumann pb	model pb
Jacobi iterations	68	34	70	35
RCS relative error	1.18%	0.92%	0.30%	0.23%

Some numerical tests have been performed for studying the influence of the frequency and of the preconditioner. Several conclusions are reported here. Concerning the solution of system (93), SymmLQ appears to be the best, in term of CPU time and number of iterations, among the other iterative methods. For instance, if a tolerance criterium is set to 10^{-4}, we present some results for Jacobi iterations as a function of SymmLQ, DbleCG or OrthoCG.

	Regular meshing with 20 points/λ			
frequency		SymmLQ	DbleCG	OrthoCG
$k = 8$	Jacobi iterations	74	74	74
	CPU time	36 s 5	1 min 20 s	41 s 68
$k = 12$	Jacobi iterations	82	82	82
	CPU time	2 min s	3 min 46 s	2 min 24 s
$k = 20$	Jacobi iterations	93	94	93
	CPU time	8 min 20 s	16 min 39 s	10 min 40 s

The CPU time is relative to a Power Challenge. It is important to notice the correlation between the frequency value and the Jacobi convergence: if the frequency is increased so is the number of required Jacobi iterations but the dependence is far less than linear.

Concerning irregular meshings, we have concluded that the inverse of the mass matrix is a good, easy to compute and reliable preconditioner for the SymmLQ algorithm. It reduces the number of SymmLQ iterations to the one in the regular case.

$k = 10$	Irregular meshing		Regular meshing
	No precond.	Mass inverse	No precond.
SymmLQ iterations	30	19	19
Jacobi iterations	78	78	78

7.4. Elliptic geometry

In the present section, we focus on elliptic geometry to observe curvature effects. We consider an ellipse characterized by semi-axis $a = 1$ and $b = 0.5$. The Helmholtz problem is solved successively with $k = 5$, $k = 10$, $k = 20$ and $k = 40$ and two kind of impedance boundary conditions are set on the boundary: either $\mathcal{R} = 1$ the **Neumann problem** or the **model problem** with $\mathcal{R} = 0$. In each case, the RCS, computed using the classical method of Integral Equations (IE) with LU inverse, is compared with the RCS obtained with our algorithms. We also report the number of iterations required by SymmLQ and by Jacobi. This emphasizes the influence of the frequency. These numerical experiments show that Jacobi convergence is better when the reflection coefficient $\mathcal{R}$ is close to 0, the model problem converges more quickly than the Neumann problem (the tolerance criterium for Jacobi residual is equal to 10^{-4}).

First $k = 5$ and the discretization is done with a regular meshing. Because we solve several iterative systems, the number of iterations refers to a mean value, for that reason a range may sometimes be given in the following tables.

Regular meshing of ellipse (200 points and 18 modes)			
frequency		$\mathcal{R} = 1$	$\mathcal{R} = 0$
$k = 5$	SymmLQ iterations	$36 - 37$	$35 - 36$
	Jacobi iterations	64	27

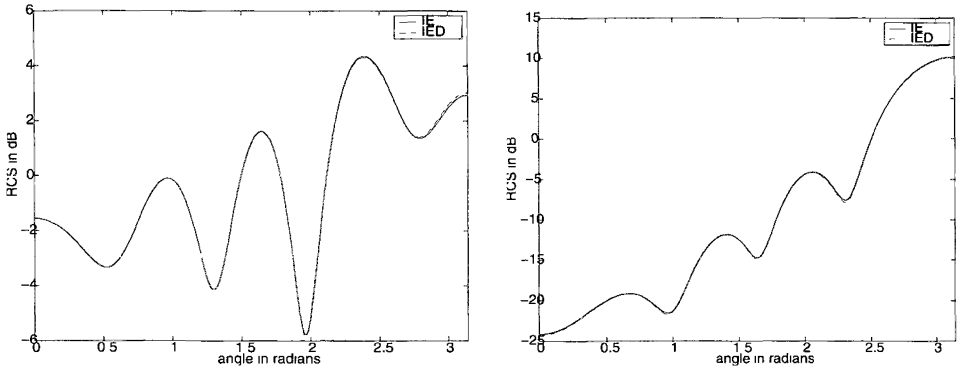

(a) $\mathcal{R} = 1$ (b) $\mathcal{R} = 0$

FIGURE 1. Comparison of the bistatic RCS of the elliptic obstacle for $k = 5$. The solid line corresponds to classical Integral Equations (IE) and the dashed line to Després Integral Equations (IED).

We perform the same tests but with an irregular mesh on the elliptic boundary.

Irregular meshing of ellipse (200 points and 18 modes)			
frequency		$\mathcal{R} = 1$	$\mathcal{R} = 0$
$k = 5$	SymmLQ iterations	$54 - 56$	$53 - 56$
	Jacobi iterations	64	27

In this elliptic case, preconditioning by the inverse of the mass matrix does not allow us to recover the number of SymmLQ iterations relative to regular meshing. However, the number of SymmLQ iterations decreases from 85-91 to 54-56 with the use of inverse of the mass matrix. So, this preconditioner saves more than 30 iterations. Table 1 sums up the convergence of SymmLQ and of Jacobi algorithm when frequency increases. For the

particular case $k = 40$, Figure 2 plots the RCS of both Neumann and model problems, and Figure 3 illustrates that the Neumann problem requires more iterations to reach tolerance criterium 10^{-4}.

TABLE 1. Number of SymmLQ and Jacobi iterations as a function of frequency if tolerance criterium is equal to 10^{-4}.

Regular meshing of ellipse: 400 points and 25 modes			
frequency		$\mathcal{R} = 1$	$\mathcal{R} = 0$
$k = 10$	SymmLQ iterations	35 – 37	32 – 35
	Jacobi iterations	76	28
500 points and 39 modes			
frequency		$\mathcal{R} = 1$	$\mathcal{R} = 0$
$k = 20$	SymmLQ iterations	24 – 25	25 – 26
	Jacobi iterations	92	30
1000 points and 63 modes			
frequency		$\mathcal{R} = 1$	$\mathcal{R} = 0$
$k = 40$	SymmLQ iterations	26	26
	Jacobi iterations	111	30

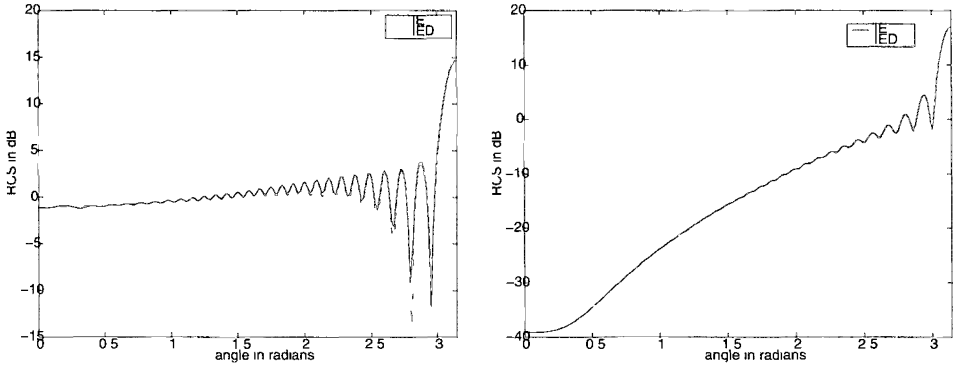

(a) $\mathcal{R} = 1$ (b) $\mathcal{R} = 0$

FIGURE 2. Bistatic RCS of elliptic obstacle for $k = 40$.

On elliptic geometry, curvature does not slow down Jacobi convergence.

7.5. Square geometry

If the scatterer is taken to be a square, the conclusions are the same as in the previous section. The algorithms of Jacobi and SymmLQ are not affected by corner effects. Moreover, the number of iterations for SymmLQ depends very weakly on the frequency whereas Jacobi iterations number increases more significantly with frequency, see Table 2.

7.6. Obstacle coated by a dielectric layer

The problem of scattering of a wave by a perfectly conducting obstacle coated by a thin dielectric layer is of interest. It is usually solved by using an impedance boundary condition to approximate the effects of the thin

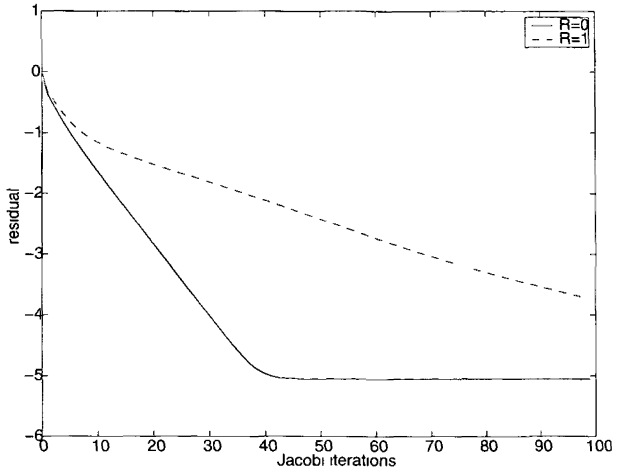

FIGURE 3. Jacobi convergence of both the model problem and the Neumann problem for $k = 40$.

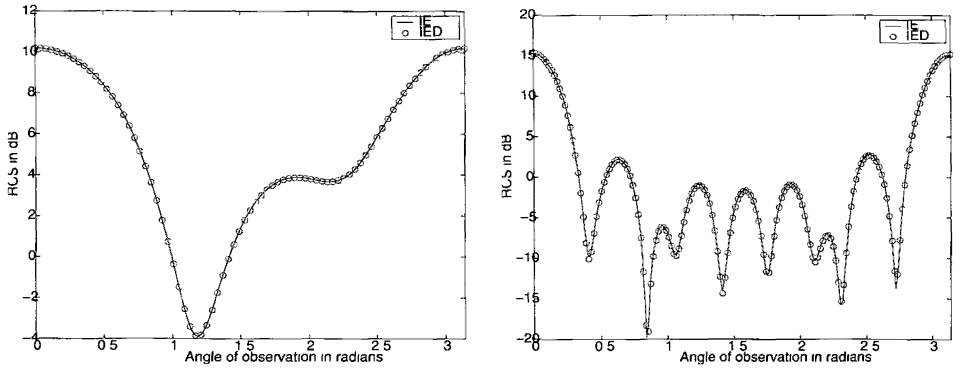

(a) $k = 2$ (b) $k = 8$

FIGURE 4. Bistatic RCS for the square geometry

TABLE 2. Number of Jacobi iterations as a function of frequency with tolerance criterium equals to 10^{-4}.

	Square	
frequency		SymmLQ
$k = 1$	Jacobi iterations	57
	CPU time (PC)	0 mn 0 s 48
$k = 5$	Jacobi iterations	57
	CPU time (PC)	0 mn 12 s 22
$k = 10$	Jacobi iterations	78
	CPU time (PC)	18 s 20

shell. For instance, these effects can be incorporated through some effective boundary condition in the form

$$\begin{cases} \partial_\nu u + ik\mathcal{Z}u = 0 \\ \mathcal{Z}\varphi = \partial_s\alpha(x(s))\partial_s\varphi + \beta(x(s))\varphi, \end{cases} \tag{100}$$

where s is the curvilinear coordinate, *cf.* [4] and [3]. Coefficients α and β depend on various parameters (wave number, curvature of the scatterer, thickness and permittivity of the thin layer).

Dealing with this kind of conditions is far from being an easy task. Here, we use the Jacobi algorithm given in Section 6 to solve (90). It mainly amounts to solve system (93) at each iteration p. As $\mathcal{C}_\beta$ does not depend on the boundary condition, the system to be inverted remains unchanged. The only thing to do is to compute the second term $\mathcal{R}_{\mathcal{R},\beta}\left[x^{p-1}, y^{p-1}\right]'$ in (93). A look at definitions (92) and (88) shows that it consists in computing $g = \mathcal{R}f^{p-1}$, f^{p-1} known and $\mathcal{R}$ given by (84). Finally, we have to solve $g + \mathcal{Z}g = f^{p-1} - \mathcal{Z}f^{p-1}$. Without going into further detail, it is important to point out that the computation of $\mathcal{R}$ requires careful attention if $\mathcal{R}$ defined in (84) is expressed as a ratio of differential operator

$$\mathcal{R} = \frac{P(\partial_s)}{Q(\partial_s)}.$$

The product matrix-vector $\mathcal{R}X$ is most easily found by splitting up the calculus into two steps

$$\mathcal{R}X = P(\partial_s)Y \quad \text{where} \quad Q(\partial_s)Y = X.$$

Indeed, after discretization these two linear systems are sparse and can be solved very easily using a QMR method [16]. Figure 5 illustrates the scattering effects of a circular dielectric layer characterized by $h = 0.05$, $\varepsilon = 2$ and $k = 5$. The solution is compared to the one obtained by the method presented in [3]. Results are in a good agreement.

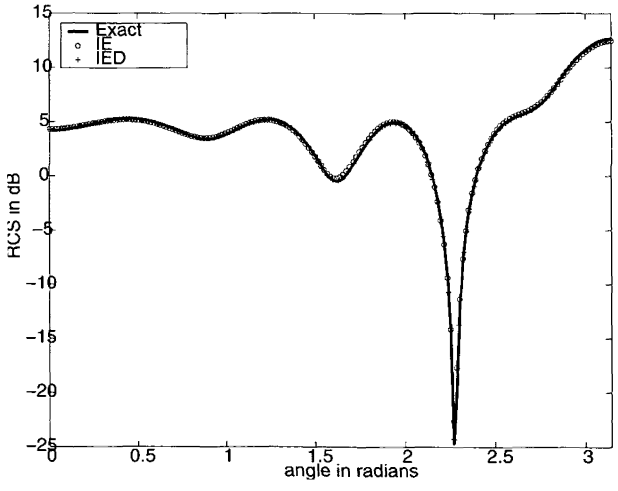

FIGURE 5. Bistatic RCS for the circular obstacle coated by a dielectric layer. The exact solution is compared with two approximated results (second order boundary condition as defined in (100) solved by Integral Method : IE or IED).

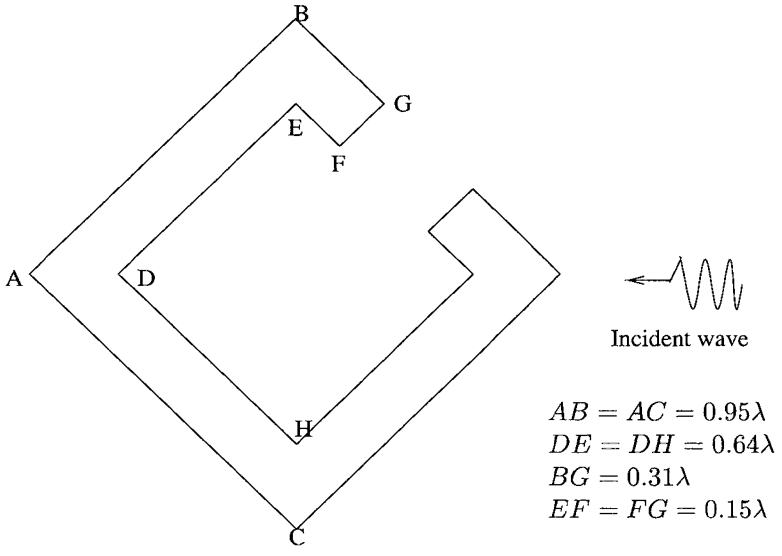

FIGURE 6. Non-convex geometry with an incidence of 45 degrees and $\lambda = 2\pi$.

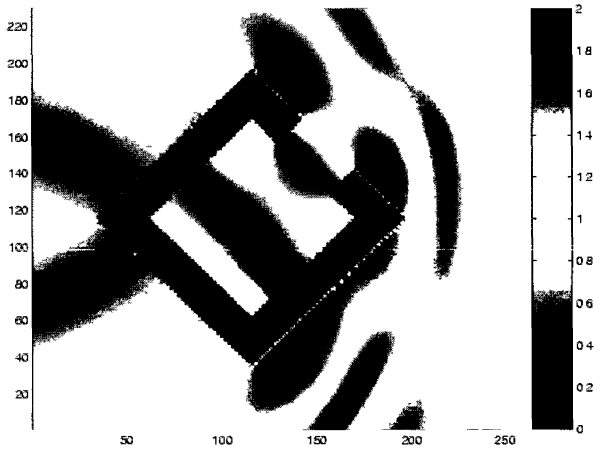

FIGURE 7. Amplitude of the electromagnetic field scattered by a perfectly conducting resonator ($k = 1$).

7.7. A non-convex geometry

Now a more complex situation is investigated. It consists in tackling a quasi-cavity problem as illustrated in Figure 6. The wavenumber k is 1 and the Neumann condition is retained. The near field is visualized in Figure 7.

For this particular geometry, some difficulties appear with the Jacobi algorithm for some angles of incidence, for instance when $\theta = 45^o$. A very slow convergence has been observed, see Jacobi's residual in Figure 8-a. The reason for the stagnation of the Jacobi residual is probably linked to the fact that the currents interior to the non-convex geometry do not radiate at infinity (as a matter of fact, stopping the Jacobi iteration at $p = 100$ provides an accurate RCS and the associated residual is 0.026). The idea is to replace Jacobi by a GMRES algorithm. In Figures 9-a and 9-b, we compare $\Re e(ku)$ of IE to the current obtained by the Jacobi method after

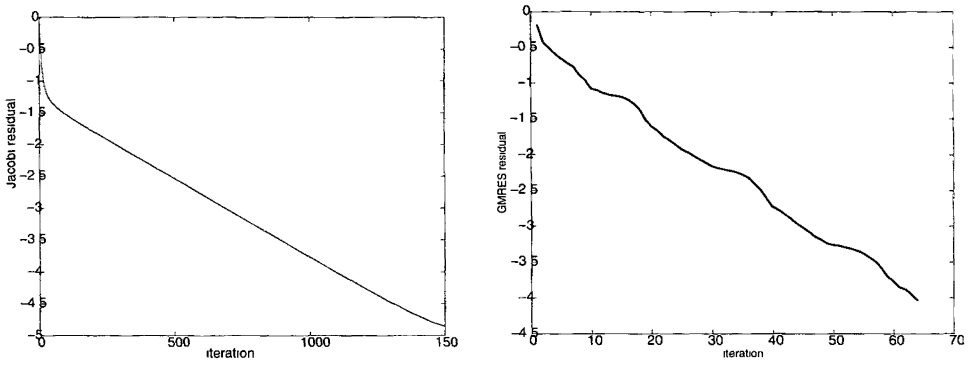

(a) Jacobi's residual (b) GMRES's residual

FIGURE 8. Residual for two different algorithms.

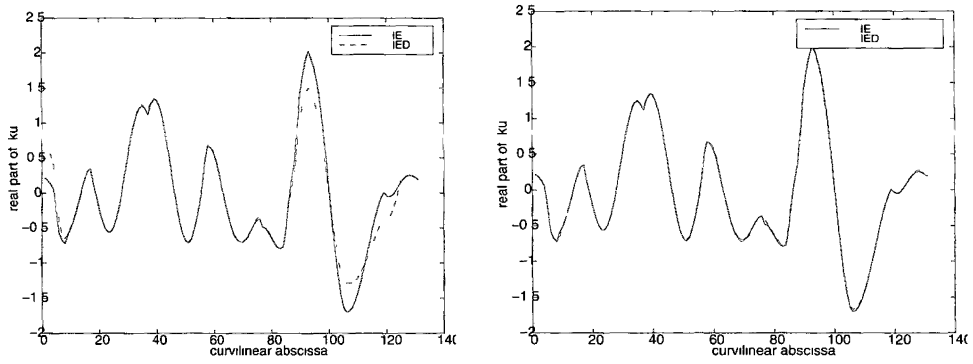

(a) IE and Jacobi (b) IE and GMRES

FIGURE 9. Real part of the current on the boundary of the resonator.

100 iterations and the GMRES method. The computation is performed with 20 points per wavelengths. Only the GMRES algorithm rapidly provides the right solution with 64 iterations if the tolerance criterium is set to 10^{-4} and the restart parameter fixed at 10, see Figure 8-b.

8. CONCLUSION

Després equations have been obtained using two different techniques. The method has been implemented and validated on several geometries. Numerical experiments have been performed with different iterative algorithms like the Jacobi or GMRES algorithms. At each iterative step, a system with a symmetric but not positive matrix must be solved and the method of SymmLQ is particularly appropriate. This iterative solver with two iteration loops proved to be effective for convex geometry. In this case, good behaviour is observed when frequency increases or when the mesh is irregular. For dielectric-covered obstacle, computation and convergence are very efficient. As regards a non-convex geometry, the determination of currents proves to be difficult and the preconditioned GMRES algorithm is suitable to cope with this particular geometry. At the end of this analysis,

it is, however, necessary to point out that the number of unknowns is four-fold with regards to classical integral equations. This is the main drawback of the method. On the other hand, the efficiency of this method for implementating impedance boundary conditions is clear. The second fundamental application, which has not been developed here, concerns a domain decomposition method [11] which benefits from the good properties of Després system.

Acknowledgements. The authors thank the CEA/CESTA and particularly J. Ovadia and the electromagnetic team for having supported this study. They would like to extend their grateful thanks to P. Monk for his careful reading of the manuscript. The authors are deeply grateful to the reviewers for meticulous reading about the manuscript and making several useful remarks.

Appendix A. The far field operator

We intend to prove the following equality

$$\int_C \mathbf{A}_\infty \begin{bmatrix} ku \\ \partial u \end{bmatrix} \overline{\mathbf{A}_\infty \begin{bmatrix} kv \\ \partial v \end{bmatrix}} \mathrm{d}\hat{x} = \int_\Gamma \mathbf{M} \begin{bmatrix} ku \\ \partial u \end{bmatrix} \overline{\begin{bmatrix} kv \\ \partial v \end{bmatrix}} \mathrm{d}\Gamma. \tag{101}$$

We start with the Jacobi-Anger relation for plane waves

$$e^{-ik\hat{x}.y} = \sum_{\ell=-\infty}^{+\infty} (-i)^\ell J_\ell(k|y|) e^{i\ell(\theta_y - \theta_{\hat{x}})}. \tag{102}$$

The relation (23) can be expanded in Fourier series

$$\begin{aligned} \mathbf{A}_\infty \begin{bmatrix} ku \\ \partial u \end{bmatrix} &= -k\sqrt{\frac{i}{8\pi k}} \sum_{\ell=-\infty}^{+\infty} (-i)^\ell \frac{2}{\sqrt{k}} (-A_D^\ell(ku) + A_S^\ell(\partial u))\, e^{-i\ell\theta_{\hat{x}}} \\ &= \sqrt{\frac{i}{2\pi}} \sum_{\ell=-\infty}^{\ell=+\infty} (-i)^\ell (A_D^\ell(ku) - A_S^\ell \partial u) e^{-i\ell\theta_{\hat{x}}} \end{aligned} \tag{103}$$

where the coefficients A_S^ℓ and A_D^ℓ are defined by

$$A_S^\ell \varphi = \frac{\sqrt{k}}{2} \int_\Gamma J_\ell(k|y|) e^{i\ell\theta_y} \varphi(y)\, \mathrm{d}\Gamma(y) \tag{104}$$

$$\begin{aligned} A_D^\ell \varphi &= \frac{\sqrt{k}}{2} \int_\Gamma J'_\ell(k|y|) \frac{y}{|y|}.\nu(y) e^{i\ell\theta_y} + \frac{i\ell}{k} J_\ell(k|y|) \nabla\theta_y.\nu(y) e^{i\ell\theta_y} \varphi(y)\, \mathrm{d}\Gamma(y) \\ &= \frac{\sqrt{k}}{2} \int_\Gamma \frac{1}{k} \partial_{\nu_y} J_\ell(k|y|) e^{i\ell\theta_y} \varphi(y)\, \mathrm{d}\Gamma(y). \end{aligned} \tag{105}$$

Using Parseval's equality, we obtain

$$\int_C \mathbf{A}_\infty \begin{bmatrix} ku \\ \partial u \end{bmatrix} \overline{\mathbf{A}_\infty \begin{bmatrix} kv \\ \partial v \end{bmatrix}} \mathrm{d}\hat{x} = \sum_{\ell=-\infty}^{\ell=+\infty} (A_D^\ell(ku) - A_S^\ell(\partial u)) \overline{(A_D^\ell(kv) - A_S^\ell(\partial v))}.$$

At this point in the proof, we have to recognize

$$\int_\Gamma \mathbf{M} \begin{bmatrix} ku \\ \partial u \end{bmatrix} \overline{\begin{bmatrix} kv \\ \partial v \end{bmatrix}} \mathrm{d}\Gamma \text{ with } \mathbf{M} = \begin{bmatrix} T_i & -K_i' \\ -K_i & S_i \end{bmatrix}.$$

The calculation has to be done for each block of the matrix. For instance, to identify S_i from $\sum_\ell A_S^\ell \ \overline{A_S^\ell}$, relations (5), (8) and (12) are used, S_i is given by

$$\int_\Gamma (S_i\varphi)(x)\overline{\varphi}(x)\ \mathrm{d}\Gamma(x) = \frac{k}{4}\int_\Gamma\int_\Gamma J_0(k|x-y|)\varphi(x)\overline{\varphi}(x)\ \mathrm{d}\Gamma. \tag{106}$$

The series development of the Bessel function J_0 is given by Graf's addition theorem, [1] page 363.

$$J_0(k|x-y|) = \sum_{\ell=-\infty}^{\ell=+\infty} J_\ell(k|x|)J_\ell(k|y|)e^{i\ell(\theta_x-\theta_y)}. \tag{107}$$

It then requires only some substitutions to obtain the identification

$$\begin{aligned}\sum_\ell A_S^\ell(\partial u)\overline{A_S^\ell}(\partial v) &= \frac{k}{4}\sum_\ell \int_\Gamma J_\ell(k|x|)e^{i\ell\theta_x}\partial u\ \mathrm{d}\Gamma \int_\Gamma J_\ell(k|y|)e^{-i\ell\theta_y}\overline{\partial v}\ \mathrm{d}\Gamma \\ &= \frac{k}{4}\int_{\Gamma\times\Gamma}\sum_\ell J_\ell(k|x|)J_\ell(k|y|)e^{i\ell(\theta_x-\theta_y)}\partial u\overline{\partial v}\ \mathrm{d}\Gamma = \int_\Gamma S_i\partial u\overline{\partial v}\ \mathrm{d}\Gamma.\end{aligned}$$

Similar calculations provide the identification for the three other blocks.

Appendix B. The asymptotic behavior of Herglotz wave functions

Let γ is in $L^2(\mathcal{C})$ we define

$$H(\gamma;x) = \sqrt{\frac{i}{8\pi k}}\int_{\mathcal{C}} \gamma(\hat{s})e^{ikx\ \hat{s}}\mathrm{d}\mathcal{C}(\hat{s}) \tag{108}$$

where $\hat{s} = e^{i\theta_{\hat{s}}} \in \mathcal{C}$.

If γ is more regular than L^2, say C^1, we can apply the stationary phase theorem to get

$$\begin{cases} H(\gamma;x) = H(\gamma;x)^{asy}\left(1+\mathcal{O}(\dfrac{1}{k|x|})\right) \\ H(\gamma;x)^{asy} = \gamma(\hat{s})\dfrac{e^{ik|x|}}{2k\sqrt{|x|}} + i\gamma(-\hat{s})\dfrac{e^{-ik|x|}}{2k\sqrt{|x|}}. \end{cases} \tag{109}$$

The problem we address here is to get some convergence result of $H(\gamma;x)$ to $H(\gamma;x)^{asy}$ for a large x when γ is less regular, in particular only in L^2.

For such a γ, we have a Fourier expansion

$$\gamma(\hat{s}) = \sum_\ell \hat{\gamma}_\ell e^{i\ell\theta_{\hat{s}}} \tag{110}$$

with

$$\hat{\gamma}_\ell = \frac{1}{2\pi}\int_{\mathcal{C}} \gamma(\hat{s}) e^{-i\ell\theta_{\hat{s}}} \mathrm{d}\mathcal{C}(\hat{s}). \tag{111}$$

By Parseval's equality, the coefficients satisfy

$$\|\gamma\|^2_{L^2} = 2\pi \sum |\hat{\gamma}_n|^2 < +\infty. \tag{112}$$

From the Jacobi-Anger expansion

$$e^{ikx.\hat{s}} = \sum_{\ell=-\infty}^{+\infty} (i)^\ell J_\ell(k|x|) e^{i\ell(\theta_x - \theta_{\hat{s}})} \tag{113}$$

we obtain easily

$$H(\gamma; x) = \sqrt{\frac{i\pi}{2k}} \sum_\ell (i)^\ell J_\ell(k|x|) e^{i\ell\theta_x} \hat{\gamma}_\ell. \tag{114}$$

Now we have the expansion

$$H(\gamma; x)^{asy} = \frac{\sqrt{i}}{k\sqrt{|x|}} \sum_\ell (i)^\ell \hat{\gamma}_\ell \cos(k|x| - \ell\frac{\pi}{2} - \frac{\pi}{4}) e^{i\ell\theta_x}. \tag{115}$$

Then we form, if R is a large number,

$$I(R) = \frac{1}{R}\int_R^{2R}\int_0^{2\pi} |H(\gamma; x) - H(\gamma; x)^{asy}|^2 |x| \mathrm{d}x\mathrm{d}\theta \tag{116}$$

$$= \frac{2\pi}{k} \sum_{\ell=-\infty}^{+\infty} |\hat{\gamma}_\ell|^2 A_\ell(R) \tag{117}$$

with

$$A_\ell(R) = \frac{1}{R}\int_R^{2R} \left| \sqrt{\frac{\pi}{2}} J_\ell(k|x|) - \frac{\cos(k|x| - \ell\frac{\pi}{2} - \frac{\pi}{4})}{\sqrt{k|x|}} \right|^2 |x| \mathrm{d}x\mathrm{d}\theta.$$

Using both asymptotic behavior

$$J_\ell(k|x|) = \sqrt{\frac{2}{\pi k|x|}} \left(\cos(k|x| - \ell\frac{\pi}{2} - \frac{\pi}{4}) + \mathcal{O}(\frac{1}{k|x|}) \right) \tag{118}$$

and the uniform bound (*via* a similar theorem to the 3D theorem of [10], p. 61)

$$\sup_\ell \frac{1}{R}\int_R^{2R} k|x| \ |J_\ell(k|x|)|^2 \mathrm{d}x < M_0 \tag{119}$$

M_0 being independent of R, we can easily conclude that

$$\lim_{R\to\infty} A_\ell(R) = 0.$$

Hence, the convergence of $H(\gamma; x)$ to $H(\gamma; x)^{asy}$ is deduced by use of the theorem of dominated convergence.

REFERENCES

[1] M. Abramowitz and I.A. Stegun, *Handbook of mathematical functions.* Dover Publications, New-York (1972).

[2] N. Bartoli, *Higher Order Effective Boundary Conditions for Perfectly Conducting Scatterers Coated by a thin Dielectric Layer.* PhD thesis, INSA, Toulouse (to appear).

[3] N. Bartoli and A. Bendali, *Higher order effective boundary conditions for perfectly conducting scatterers coated by a thin dielectric layer and their boundary element solution* (to be submitted).

[4] A. Bendali, Boundary element solution of scattering problems relative to a generalized impedance boundary condition, in *Partial differential equations, Theory and numerical solution*, W. Jäger, J. Nečas, O. John, K. Najzar and J. Stará, Eds. Chapman & Hall/CRC, **406** (1999) 10–24.

[5] A. Bendali and L. Vernhet, Résolution par élements finis de frontière d'un problème de diffraction d'onde comportant une condition aux limites d'impédance généralisée. *C. R. Acad. Sci. Paris*, **321** (1995) 791–797.

[6] F. Brezzi and M. Fortin, in *Mixed and Hybrid Finite Element Method*, volume 15, Springer-Verlag (1991).

[7] D. Calvetti, L. Reichel and Q. Zhang, Conjugate gradient algorithms for symmetric inconsistent linear systems. in *Proceedings of the Cornelius Lanczos International Centenary Conference*, J.D. Brown, M.T. Chu, D.C. Ellison and R.J. Plemmons, Eds. SIAM, Philadelphia (1994) 267–272.

[8] G. Chen and J. Zhou, in *Boundary element Methods.* Academic Press, London (1992).

[9] F. Collino and B. Després, Integral equations *via* saddle point problems for time-harmonic Maxwell's equations. *SIAM J. Appl. Math.* (submitted).

[10] D. Colton and R. Kress, in *Inverse Acoustic and Electromagnetic Scattering Theory*, **93**, Springer-Verlag (1992).

[11] B. Després, Quadractic functional and integral equations for harmonic wave problems in exterior domains. RAIRO-Modél. Math. Anal. Numér. **31** (1997) 679–732.

[12] V. Frayssé, L. Giraud and S. Gratton, A set of GMRES routines for real and complex arithmetics. Technical report, Cerfacs TR/PA/97/49, Toulouse, France (1997).

[13] V. Girault and P.A. Raviart, in *Finite Element methods for Navier-Stokes Equations, Theory and Algorithms*, **5**, Springer-Verlag (1986).

[14] G.H. Golub and C.F. Van Loan, in *Matrix Computations*, 3rd edn., Chap. 9-10, The Johns Hopkins University Press, Baltimore (1996).

[15] B. Perthame and L. Vega, Morrey-Campanato estimates for Helmholtz equations. *J. Funct. Anal.*, **164** (1999) 340–355.

[16] Y. Saad, in *Iterative methods for sparse linear systems.* PWS publishing (1995).